INSTITUTE OF PHYSICS PUBLISHING NANOTECHNOLOGY
Nanotechnology **17** (2006) 4477–4482 doi:10.1088/0957-4484/17/17/032

Synthesis of silicon quantum dot buried SiO_x films with controlled luminescent properties for solid-state lighting

Z T Kang[1,2,3], B Arnold[4], C J Summers[2,3] and B K Wagner[1,2]

[1] Georgia Tech Research Institute, Georgia Institute of Technology, Atlanta, GA 30332, USA
[2] Phosphor Technology Center of Excellence, Georgia Institute of Technology, Atlanta, GA 30332, USA
[3] School of Materials Science and Engineering, Georgia Institute of Technology, Atlanta, GA 30332, USA
[4] Fort Valley State University, Fort Valley, GA 31030, USA

Received 26 June 2006, in final form 25 July 2006
Published 21 August 2006
Online at stacks.iop.org/Nano/17/4477

Abstract
Highly luminescent Si quantum dot embedded SiO_x films were studied as down-converting emitters for solid-state lighting applications. Strong red photoluminescence was observed from these Si nanocrystal embedded films prepared by thermal evaporation of SiO in vacuum or an O_2 atmosphere followed by anneal at 1100 °C. The stoichiometry ($1.0 < x < 1.9$) and refractive indices (1.5–1.75) of these films could be well controlled by varying the oxygen flow rate and the deposition rate. The emission peak shifted from 840 to 745 nm with increasing O_2 flow rate due to a decrease in the size of the Si QDs. Two excitation bands, peaked at 280 and 370 nm, were observed from these samples. The 370 nm band was much stronger than the 280 nm band, which is near the UV LED emission range required for solid-state lighting applications. Blue and green emissions were also observed from samples annealed at a lower temperature.

1. Introduction

Light emission from silicon quantum dots (QDs) has attracted much attention due to its potential for low cost Si-based optoelectronic devices [1–6], especially when synthesized by methods compatible with Si microelectronics technology. Luminescent Si QDs which are embedded in a matrix of oxide or nitride have been synthesized by various techniques. Typical techniques reported for preparing Si QD embedded films include plasma-enhanced chemical vapour deposition (PECVD) [7–10], thermal or electron-beam evaporation [11–14], magnetron sputtering [15], and ion implantation [16].

LED-based solid-state lighting (SSL) exhibits higher energy conversion efficiency and longer life with compact structure compared to conventional lamps, and in recent years has attracted intense research [17–19]. White LEDs can be fabricated by coating down-converting phosphors onto a blue/UV LED to emit white light [18, 19]. Si QDs can emit throughout the visible by controlling their size and/or the host matrix. Consequently, multiple coloured (size) Si QDs embedded in thin films can be used to produce efficient white light sources with controlled spectrum characteristics when integrated with a blue/UV LED and film structures designed for high light extraction. Thin film Si QDs are very stable and non-scattering, and can be tailored to match refractive indices in the range of 1.44–2. Thus, it becomes easier to engineer their light output distribution than with traditional, scattering phosphors. Moreover, a Si-based microelectronics compatible technology can be developed through the application of thin film QDs, providing a continuous, more efficient and less expensive fabrication process to obtain advanced white light emitting SSL devices with a sunlight spectrum.

SSL therefore requires highly efficient down-converting emitters which can be strongly excited by 280–470 nm GaN-based UV/blue LED. However, little information has been reported on the photoluminescence excitation (PLE) properties of thin film Si QDs. In this research, the PLE properties as well as photoluminescence (PL) of thin film Si QDs were evaluated for SSL application. Although quantum efficiencies (QE) up

to 88% have been reported from single Si nanoparticles at room temperature [20], the reported external QE of thin film Si nanoparticles was much lower. For example, Wang *et al* reported 0.5–5% QE from red to blue emitting Si nanoparticles embedded in SiN_x films [21]. These lower efficiencies are probably due to thin film entrapment effects and a statistic distribution of the QE of individual QDs resulting from different quantum confinement and passivation conditions. However, through the use of engineered optical structures, such as textured surfaces, microcavities, antireflection coatings, filters, and Bragg reflectors, the light extraction efficiency from the QD thin films can be significantly improved [1]. This implies that highly efficient engineered optical Si QD structures are achievable for SSL. In this research, efficient red emitting thin film Si QDs were systematically studied using an industrial ion assisted deposition (IAD) system, which provides superior coating material quality with great layer thickness control for various optical structures. Refractive indices and stoichiometry of these films were controlled and studied, providing useful information for further integration of these films with engineered optical structures to improve the out-coupling efficiency.

2. Experimental details

2.1. Synthesis

SiO_x ($x \sim 1$–1.9) films were deposited by thermal evaporation of SiO from a molybdenum boat using a highly automated IAD system (Leybold APS 1104). Silicon(100) or quartz substrates were used and the substrate temperature during deposition was maintained at 50 °C. The films were deposited at a background pressure of $\sim 3 \times 10^{-6}$ mbar in the presence of a reactive gas atmosphere, O_2, for flow rates between 0 and 35 sccm. The deposition rate (0.2–2.5 nm s^{-1}) was controlled by a calibrated quartz microbalance system, which allowed the automatic adjustment of power level applied on the source material. The film thicknesses were set at 300 nm. After deposition, the films were annealed in a quartz tube at 300–1100 °C from 5 min to 72 h in a N_2 or 96% N_2/4% H_2 atmosphere by rapidly inserting the gas-purged tube into a furnace preheated to the desired temperature.

2.2. Characterization

The as-deposited SiO_x films were characterized by optical reflectance and energy dispersive x-ray spectroscopy (EDXS) measurements to obtain the refractive index, thickness and composition. The physical structure, dimensions, and size of the Si QDs were analysed by a LEO 1530 scanning electron microscope (SEM) and a high resolution JEOL 4000EX transmission electron microscope (HRTEM) operated at 400 kV. Surface chemical analysis was performed using a Surface Science model SSX-100 Small Spot ESCA x-ray photoelectron spectroscopy (XPS) system using the Al Kα line (1486.6 eV). The photoluminescence (PL) and photoluminescence excitation (PLE) spectra were obtained with a Spex1000M spectrometer using a 450 W xenon lamp/monochromator combination as the excitation source. Some PL spectra were measured using the 275 nm UV line of an argon laser at a power of 5 mW as the excitation source.

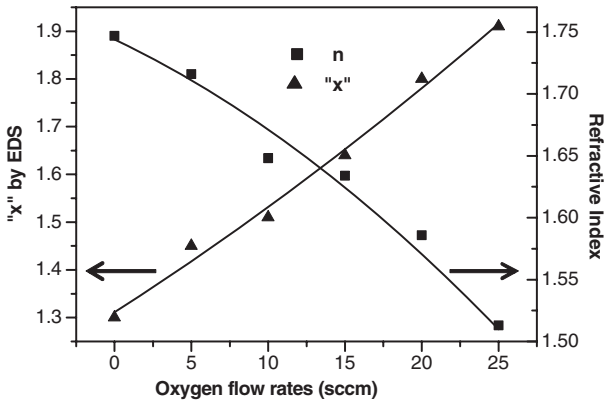

Figure 1. Dependence of refractive index and stoichiometry of as-deposited SiO_x films as a function of oxygen flow rates for constant SiO deposition rate: 0.2 nm s^{-1}.

All the PL measurements were performed at room temperature and recorded with a GaAs photomultiplier tube (PMT) which cuts off at 920 nm. The QE of samples on quartz substrates were measured using an integrating sphere connected to an Ocean Optics USB2000 spectrometer with the argon laser as the excitation source. The sample was face down, on top of the hole of the integrating sphere, with the laser beam going through the substrate and film into the sphere. Thus, the integrated emission intensity from the bottom hemisphere of the film sample could be measured by the spectrometer. The UV power absorbed by the film sample was estimated using a Spectra-Physics 407A power meter.

3. Results and discussion

3.1. Stoichiometry and microstructure

A series of amorphous SiO_x films was prepared by thermal evaporation of SiO in a controlled O_2 atmosphere. The film stoichiometry was well controlled by adjusting the oxygen flow rate and the SiO deposition rate. As shown in figure 1, at a fixed deposition rate of 0.2 nm s^{-1}, the x-value increased from 1.3 to 1.9 with increasing oxygen flow rate from 0 to 25 sccm, due to the higher reaction rate of silicon with oxygen at higher oxygen partial pressures. It is well known that by controlling the x ratio of the SiO_x films, their refractive indices can be adjusted from $\sim$1.5 (index of SiO_2) to $\sim$2 (index of SiO) [22]. Therefore, the monotonic decrease of the index from 1.75 to 1.51 with increasing oxygen flow rate, as shown in figure 1, presents evidence of the continuous change of the stoichiometry in the thin films. In addition, the deposition rate affects the stoichiometry. The higher the deposition rate, the lower the oxygen content, due to the time-limited uptake rate of oxygen. Films with x equal to $\sim$1.0 and an index of 2.0 were obtained by increasing the deposition rate to 2.5 nm s^{-1} under a high vacuum with no oxygen flow. The tunable index makes it possible to grow *in situ* light extraction structure for the LED diode. For instance, silicon oxide based anti-reflective coating, which had been used for laser diode optical amplifiers [23], could be formed on a III nitride LED while also providing a second or third colour emission band, making for a more efficient, better saturated light source.

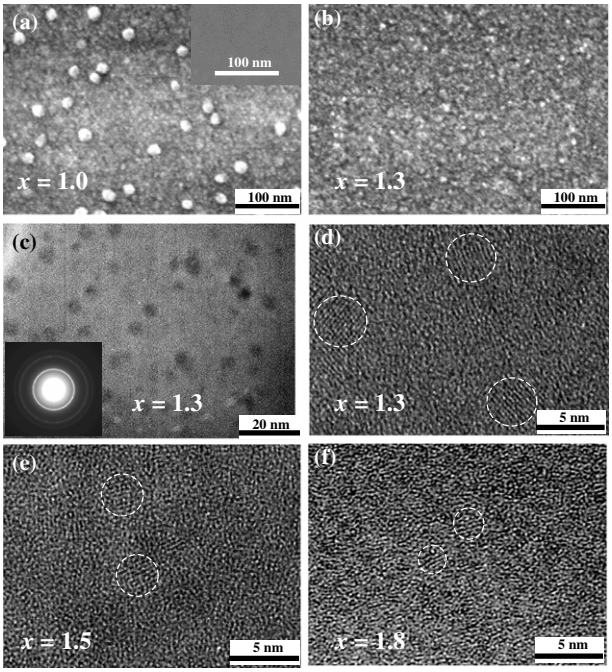

Figure 2. SEM and TEM images of SiO_x films: (a) sample with x equal to ∼1.0 and Si dots of ∼20 nm after annealing at 1100 °C for 1 h; the inset shows the as-deposited film; (b) sample with x equal to 1.3 and Si dots smaller than ∼5 nm; (c) sample with x equal to 1.3; Si QDs (darker spots) of ∼4 nm in diameter are discernible; the inset shows the electron beam diffraction pattern; (d) an HRTEM image of the same sample with x equal to 1.3; the Si QD shows lattice plane fringes indicating crystalline structure; (e) sample with x equal to 1.5 and Si QDs of ∼3 nm; (f) sample with x equal to 1.8 and Si QDs of ∼2 nm.

SEM was used to study relatively larger Si nanoparticles (>∼4 nm) which appeared on the film surface. As shown in figure 2(a), it can be observed that spherical nanoparticles ∼20 nm in diameter were formed in a silicon rich SiO_x sample with x close to 1 after annealing at 1100 °C for 1 h, but no Si dots were observed in the as-deposited SiO_x films. This confirmed that excess silicon segregated during the high temperature anneal. These Si nanoparticles were uniformly distributed across the surface area with a density of 2×10^{10} cm^{-2}. With increasing O/Si ratio, the particle size of the precipitated Si dots decreased. Figure 2(b) shows the SEM image of a sample with x equal to 1.3, indicating that Si QDs smaller than ∼5 nm were formed in the film. This decrease in the size of Si QDs is due to the lower excess silicon content in the film.

TEM studies were performed to confirm the size and structure of the Si QDs. As shown in figure 2(c), relatively darker Si QDs can be observed from the plan view TEM images of a sample with x equal to 1.3 after annealing at 1100 °C for 1 h, due to a higher atomic density than the surrounding silicon dioxide matrix. The image illustrates that Si QDs with a density of 5×10^{11} cm^{-2} are uniformly embedded within the oxide matrix, and are approximately spherical in shape, with a mean diameter of ∼4 nm. The electron beam diffraction pattern shown in the inset of figure 2(c) indicates that these Si QDs are highly crystalline. Figure 2(d) shows the high resolution TEM image of this sample. The crystallite can be recognized from its lattice plane fringes of the cubic crystal structure, which is surrounded by the amorphous silicon oxide matrix. The appearance of the nano-crystallized Si dots in the annealed sample implies that both the segregation and crystallization of Si QDs occur during the thermal process at 1100 °C. It was also observed by TEM that the size and density of Si QDs decreases with increasing oxygen content in the films. As shown in figures 2(e) and (f), Si QDs of ∼3 and ∼2 nm in diameter were observed from thin films with x equal to 1.5 and 1.8, respectively.

3.2. Photoluminescence properties

When excited by 275–380 nm UV light, the 1100 °C annealed SiO_x films with indices less than 1.75 exhibited intense luminescence in the red and infrared. Figure 3(a) shows the normalized room temperature PL spectra of samples prepared under various O_2 flow rates from 0 to 25 sccm when excited by 300 nm UV from a xenon lamp. For samples 4–6 with shorter wavelength emission, the PL band usually exhibited a symmetric Lorentz shape, indicating that the emission probably originates from excitonic recombination in the buried Si QDs with a Gaussian distribution of the particle size [11]. The asymmetric shape of the PL band from samples 1–3 is due to the low responsivity of the detector at wavelengths longer than ∼900 nm. The emission band peak shifted from 840 to 745 nm with increasing O_2 flow rate and decreasing silicon content. A similar observation has also been reported by other authors [10, 11]. The blue-shift in the PL spectra is attributed to the quantum confinement effect produced by a decrease in the size of the QDs [11, 13, 21]. It was also noticed that when the O_2 flow rate was increased from 0 to 10 sccm, the relative PL intensity increased and reached a maximum, but dropped with further increase in the O_2 flow rate (not shown in figure 3(a)). This change is attributed to the competing effects caused by carrier confinement and the density of Si QDs in the SiO_x films. For samples with smaller x-values, the confinement effect becomes weaker with decreasing oxygen content and increasing nanocrystallite size, and the indirect bandgap of crystalline Si lead to a decrease in PL intensity [13]. For samples with large x-values ($x > 1.5$), the density of Si QDs decreases with increasing oxygen content or with decreasing excess Si, which also results in decrease in intensity. Therefore, the maximum intensity was obtained at a medium O_2 flow rate of 10 sccm.

PLE measurements were carried out by monitoring the intensity of the peak emission wavelength as a function of excitation wavelength. Figure 3(b) shows the PLE spectra corresponding to the samples shown in figure 3(a), between 250 and 650 nm. For all samples, above 650 nm, a continuous decrease in intensity was observed and no obvious excitation bands were evident. For samples with higher silicon content ($x > 1.5$, curves 1–4), two excitation bands peaked at ∼280 and ∼370 nm were detected. The 370 nm band was ∼1.5 times stronger than the 280 nm band, and is close to the UV LED pump wavelength (360–400 nm) required for SSL applications. Similarly, two PLE bands were also reported by Kwack *et al* [24] from amorphous Si QDs buried in a silicon nitride matrix. For samples with lower silicon content ($x < 1.5$, curves 5 and 6), the 370 nm excitation band was blue-shifted, to 360

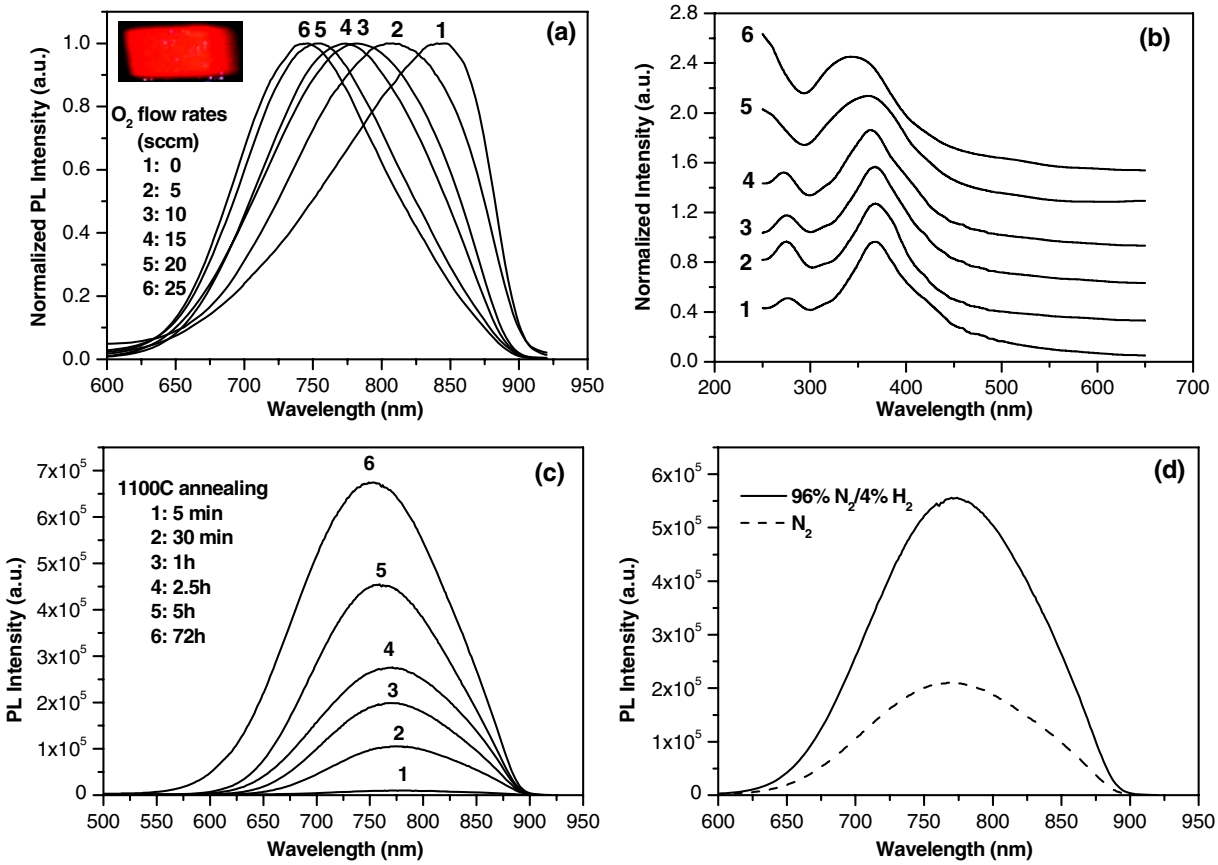

Figure 3. Normalized PL (a) and PLE (b) spectra of SiO_x films prepared with various O_2 flow rates after annealing at 1100 °C; (c) PL spectra as a function of annealing time from 5 min to 72 h at 1100 °C; (d) PL spectra of N_2 and 96% N_2/4% H_2 annealed sample after annealing at 1100 °C for 1 h.

(This figure is in colour only in the electronic version)

and 340 nm, respectively. However, the 280 nm band was not observed in these two samples, although the PLE intensity increased continuously towards shorter wavelength. The PLE band near 370 nm (3.35 eV) is attributed to the continuum states of the Si QDs, which have a large Stokes-like shift (>375 nm) related to the PL emission wavelength. The slight blue-shift of the 370 nm band with increasing oxygen content and decreasing Si QD size is probably caused by the shift of the quantized states in the Si QDs due to the quantum confinement effect.

Figure 3(c) shows the room temperature PL spectra of a sample after being annealed at 1100 °C from 5 min to 72 h. These data indicate that the PL intensity increases significantly with annealing time. Only a weak blue emission at 420 nm was observed from the as-deposited film sample, but after annealing for 5 min a deep red emission at 780 nm could be detected, indicating that preliminary segregation and crystallization of Si QDs occurred in the film. However, to obtain strong luminescence, longer annealing times were required. A factor of three increase in PL intensity was observed after a 72 h anneal compared to a 1 h anneal. Also, with increasing annealing time, the emission shifted to shorter wavelengths (from 780 to 745 nm). This was attributed to a smaller Si QD size due to the oxidation and/or nitridation of Si during prolonged high temperature annealing. Therefore, the increase in intensity with annealing time can be attributed to stronger quantum confinement due to the smaller Si QD size. In addition, the improvement in crystallinity caused by longer time annealing may also lead to higher PL intensity. To further improve the luminescent efficiency, annealing in a H_2 atmosphere was investigated. As shown in figure 3(d), after annealing in a 96%N_2/4%H_2 atmosphere at 1100 °C for 1 h, the PL intensity increased by 2.5 times that of a N_2 annealed sample, although the spectral profile and peak wavelength were unchanged, indicating that the size distribution of the QDs was not affected. The improvement in PL intensity was attributed to better passivation of the Si QDs by H_2 annealing.

The external QE of the optimized films under 275 nm UV excitation, which was limited by the thin film entrapment effects, was estimated to be ∼4% from samples deposited on quartz substrates. After excited by an argon laser, the emission intensities were measured using a calibrated integrating sphere which connected to a spectrometer; and the UV absorptions were estimated using a power meter. Thus, the QE could be calculated from the emission and absorption data. According to the PLE spectra, the efficiency at 370 nm is ∼1.7 times higher than at 275 nm. Thus the QE at 370 nm is close to 7%. This is much higher than the reported external efficiency, ∼0.5%, for the red emitting amorphous Si nanoparticle buried thin films prepared by PECVD [21]. The extraction efficiency,

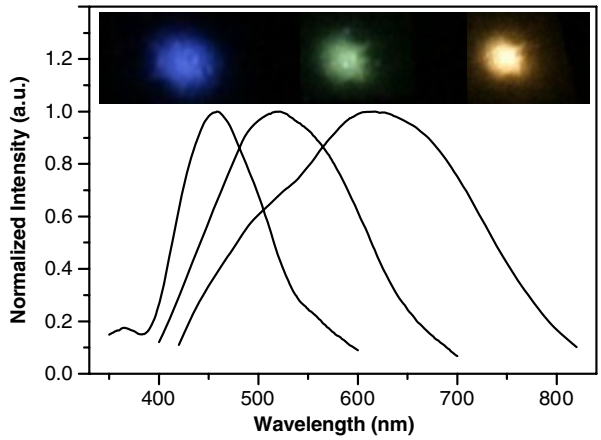

Figure 4. PL spectra of SiO_x films and corresponding images of displayed colours for 275 nm UV excitation.

η_p, of a thin film emitter can be estimated using the following equation by considering both the total internal reflection and the Fresnel reflection at the thin film–air interface [25]:

$$\eta_p = \frac{1}{2}\left(1 - \sqrt{1 - \left[\frac{1}{n_c}\right]^2}\right)\frac{4n_c}{(1+n_c)^2} \cong \frac{1}{n_c(n_c+1)^2},$$

where n_c is the refractive index of the thin film. The first term in the equation accounts for the total internal reflection and the second term represents the Fresnel transmission for normal incidence. The factor $1/2$ is used because only half of the excited radiation propagates in the direction of the emitting surface. It is evident that an increase in n_c will decrease the efficiency for light coupling from the QD layer to air. For a Si QD buried SiO_x film with n_c equal to 1.64, this equation dictates that thin film effects can limit the external efficiency of a 100% internal efficiency thin film emitter to ∼9%. Thus, the estimated external QE, 7%, from this film is approximately equivalent to an internal QE of 78%. To improve the extraction efficiency for SSL applications, further integration of these films with engineered optical structures needs to be studied.

Other visible colours were also observed from the prepared SiO_x films, as shown in figure 4. For SiO_x films annealed at 1100 °C, the shortest emission wavelength, which peaked at 620 nm with a yellow–orange colour, was obtained from a sample deposited at an oxygen flow rate of 35 sccm and with an x-value close to 2. However, the PL intensity was much weaker, an order of magnitude lower than for the sample deposited for an oxygen flow rate of 10 sccm, probably due to a very low excess Si content and density of Si QDs. In addition, by annealing at lower temperatures (500 °C), blue and green emissions were observed, which probably originated from amorphous Si QDs [26]. However, the emission was again much weaker compared to samples annealed at 1100 °C. For practical white LED applications, efficient blue and green light emitting thin film Si QDs need to be developed. This may be accomplished by the PECVD technique, in which high density amorphous Si QDs can be formed during the film deposition procedure. Thus, only a short or even no post-annealing would be needed after film deposition, avoiding significant growth of Si QDs during the high temperature annealing and excessive red-shift of PL. For example, Wang *et al* reported efficient red to blue–green PL from amorphous Si QDs in a SiO_x matrix prepared by PECVD [27]. In addition, the host matrix and the film/QD interface also play important roles in determining the PL properties of Si QDs. It seems that nitride-encapsulated Si QDs exhibit shorter emission wavelengths and more intense PL compared to oxide-encapsulated ones [21].

4. Conclusion

In conclusion, highly efficient luminescent red and infrared Si QDs embedded in SiO_x thin films were prepared by thermal evaporation of SiO in vacuum or in an O_2 atmosphere followed by annealing at 1100 °C. It was demonstrated that stoichiometry ($1.0 < x < 1.9$) and refractive indices of the SiO_x films could be well controlled by varying the oxygen flow rate and the deposition rate. Silicon nanocrystals 2–20 nm in size were formed in films with different stoichiometries. Photoluminescence with peak wavelengths ranging from 745 to 840 nm was observed from embedded crystalline Si QDs smaller than ∼5 nm in diameter. The blue-shift of the PL peak was correlated to a reduction in the particle size due to the quantum confinement effect. The PL intensity increases with the annealing time. More than a threefold improvement in the PL intensity was detected from a 72 h annealed sample compared to a 1 h anneal. By annealing in a H_2 containing atmosphere, the PL intensity was improved 2.5-fold compared to N_2 annealing. A strong PL excitation band was observed around 370 nm, close to the near UV LED emission range, and thus these Si QD thin films could be used for SSL applications.

Acknowledgments

The authors would like to thank Dr Ye Cai for the high resolution TEM measurements. This research was supported financially by the Robert G Shackelford Graduate Fellows Programme and the Summer Undergraduate Research Fellowship Programme funded by NSF DMR-0453293.

References

[1] Fauchet P M 2005 *Mater. Today* **8** 26
[2] Nishio K, Koga J, Yamaguchi T and Yonezawa F 2003 *Phys. Rev.* B **67** 195304
[3] Tong J F, Hsiao H L and Hwang H L 1999 *Appl. Phys. Lett.* **74** 2316
[4] Pei Z and Hwang H L 2003 *Appl. Surf. Sci.* **212/213** 760
[5] Wolkin M V, Jorne J, Fauchet P M, Allan G and Delerue C 1999 *Phys. Rev. Lett.* **82** 661
[6] Chan S and Fauchet P M 1999 *Appl. Phys. Lett.* **75** 274
[7] Park N M, Choi C J, Seong T Y and Park S J 2001 *Phys. Rev. Lett.* **86** 1355
[8] Park N M, Kim T S and Park S J 2001 *Appl. Phys. Lett.* **78** 2575
[9] Kim B H, Cho C H, Kim T W, Park N M, Sung G Y and Park S J 2005 *Appl. Phys. Lett.* **86** 091908
[10] Chen X Y, Lu Y F, Tang L J, Wu Y H, Cho B J, Xu X J, Dong J R and Song W D 2005 *J. Appl. Phys.* **97** 014913
[11] Kahler U and Hofmeister H 2002 *Appl. Phys.* A **74** 13
[12] Zacharias M, Heitmann J, Scholz R, Kahler U, Schmidt M and Blasing J 2002 *Appl. Phys. Lett.* **80** 661
[13] Nesheva D, Raptis C, Perakis A, Bineva I, Aneva Z, Levi Z, Alexandrova S and Hofmeister H 2002 *J. Appl. Phys.* **92** 4678
[14] Rinnert H, Vergnat M, Marchal G and Burneau A 1998 *Appl. Phys. Lett.* **72** 3157

[15] Wu X L and Xue F S 2004 *Appl. Phys. Lett.* **84** 2808
[16] Min K S, Shcheglov K V, Yang C M and Atwater H A 1996 *Appl. Phys. Lett.* **69** 2033
[17] Pearton S J, Abernathy C R, Overberg M E, Thaler G T, Onstine A H, Gila B P, Ren F, Lou B and Kim J 2002 *Mater. Today* **5** 24
[18] Zorpette G 2002 *IEEE Spectrum* **39** 70
[19] Mueller-Mach R, Mueller G O, Krames M R and Trottier T 2002 *IEEE J. Sel. Top. Quantum Electron.* **8** 339
[20] Credo G M, Mason M D and Buratto S K 1999 *Appl. Phys. Lett.* **74** 1978
[21] Wang Y Q, Wang Y G, Cao L and Cao Z X 2003 *Appl. Phys. Lett.* **83** 3474
[22] Nesheva D, Bineva I, Levi Z, Aneva Z, Merdzhanova T and Pivin J C 2003 *Vacuum* **68** 1
[23] Wecht K W 1991 Large-range refractive-index control of silicon monoxide antireflection coatings using oblique incident thermal evaporation *Appl. Opt.* **30** 4133
[24] Kwack H S, Sun Y and Cho Y H 2003 *Appl. Phys. Lett.* **83** 2901
[25] Zacharias M, Heitmann J, Yi L, Scholz R, Reiche M and Gosele U 2002 *Proc. SPIE* **4808** 28
[26] Yi L X, Heitmann J, Scholz R and Zacharias M 2003 *J. Phys.: Condens. Matter* **15** S2887
[27] Wang Y Q, Chen W D, Liao X B and Cao Z X 2003 *Nanotechnology* **14** 1235